

J80-034

# Local Turbulence Properties in Flames from Time-Averaged Raman Spectroscopy Measurements

20014  
60003  
90002

Robert E. Setchell\*

*Sandia Laboratories, Albuquerque, New Mexico*

Local fluctuations in temperature and composition in a turbulent flame are examined through their influence on Raman-scattering measurements of time-averaged flame properties. Using mean temperatures and number densities measured in a hydrogen diffusion flame, two approaches to investigating turbulence properties are examined. In the first, which is restricted to flame conditions where fluctuations are fairly small, the variation of measured number density with spectral resolution is used to determine values for particular correlations between fluctuations in number density and temperature. In the second approach, the Raman measurements are used to evaluate a particular model for concentration fluctuations. The shifting-equilibrium reaction model is combined with a clipped-Gaussian probability density function for mixture fraction in order to predict time-averaged Raman signals. Comparisons with the Raman data determine particular radial distributions for the mean mixture fraction and for the intensity of concentration fluctuations. These distributions are then used to predict a variety of averaged flame properties, as well as the errors occurring in the time-averaged Raman measurements.

## I. Introduction

**A**LTHOUGH turbulent diffusion flames are utilized in many combustion devices, investigations of these flames have not established a fundamental theoretical description from which accurate predictive models can be readily formulated. The theoretical difficulties introduced by the coupling between kinetics and turbulent eddy mechanics, together with current schemes for addressing these difficulties, are described in recent reviews.<sup>1,2</sup> An important factor restricting theoretical progress is the lack of an extensive body of experimental data from these flames. Since the early study of Hawthorne et al.,<sup>3</sup> only a few experimental studies have been reported. Kent and Bilger<sup>4</sup> used thermocouple and isokinetic sampling probes to obtain mean temperatures and concentrations in co-flowing hydrogen/air diffusion flames. Bilger and Beck<sup>5</sup> used an improved probe to obtain mean concentrations in both co-flowing hydrogen/air flames and vertical hydrogen flames into still air. The possible error mechanisms in applying these probe techniques to turbulent flames were discussed by Kent and Bilger.<sup>6</sup> Lavoie and Schlader<sup>7</sup> used a sonic sampling probe to obtain mean concentrations in vertical hydrogen flames into still air. A direct examination of turbulence fluctuations was reported by Lockwood and Odidi.<sup>8</sup> Using a fine-wire thermocouple, these authors obtained probability density functions for temperature at various axial and radial positions in a vertical methane diffusion flame.

An experimental method capable of providing non-perturbing point measurements of temperature and concentrations in turbulent flames would obviously enhance the progress of predictive models. In recent years a number of experimental studies have been reported which demonstrate the ability of Raman spectroscopy to provide local

measurements of temperature and composition in laboratory flames. The majority of these studies have involved measurements in the post-flame gases of premixed, laminar flames.<sup>9-13</sup> In one study, however, the feasibility of using a cw-laser system to obtain time-averaged Raman measurements in a turbulent diffusion flame was investigated.<sup>14</sup> Mean temperatures from both hydrogen and nitrogen spectra and the concentrations of H<sub>2</sub>, O<sub>2</sub>, and N<sub>2</sub> were obtained in a vertical diffusion flame of hydrogen into still air. This study introduced the possibility of significant errors occurring in the Raman measurements due to the fluctuations in temperature and composition at the flame position under examination. These errors arise from the dependence of measured Raman signals on both temperature and species number density. An error analysis was presented for various measurement cases, but estimates of error magnitudes were not made.

The present study again considers the effects of turbulence fluctuations in flames on time-averaged Raman signals. The objective of this study is to demonstrate that these effects can be used to obtain relevant information on local turbulence properties. The time-averaged relations between Raman signals and flame properties are reviewed in Sec. II. In this section the spectral resolution of the detection system is shown to control the degree to which Raman signals are influenced by temperature fluctuations. An analysis of time-averaged Raman signals, measured when fluctuations are small compared to mean values, is reviewed in Sec. III. The analysis suggests a method for directly determining particular correlations between number density and temperature fluctuations, and this method is tested using data obtained in the previous study of hydrogen diffusion flame.<sup>14</sup> In Sec. IV a set of time-averaged Raman measurements is shown to be a useful basis for evaluating theoretical models for concentration fluctuations. As an example, the shifting-equilibrium reaction model<sup>15,16</sup> is combined with a clipped-Gaussian form of the probability density function for mixture fraction<sup>17,18</sup> to predict time-averaged Raman signals. Comparisons with Raman data obtained in the previous study<sup>14</sup> determine particular radial distributions for the mean mixture fraction and for the intensity of concentration fluctuations. These distributions are then used to predict a variety of averaged flame properties, as well as the errors made in time-averaged Raman measurements.

Presented as Paper 79-0087 at the AIAA 17th Aerospace Sciences Meeting, New Orleans, La., Jan. 15-17, 1979; submitted Feb. 12, 1979. This paper is declared a work of the U.S. Government and therefore is in the public domain. Reprints of this article may be ordered from AIAA Special Publications, 1290 Avenue of the Americas, New York, N.Y. 10019. Order by Article No. at top of page. Member price \$2.00 each, nonmember, \$3.00 each. **Remittance must accompany order.**

Index categories: Combustion Stability, Ignition, and Detonation; Reactive Flows; Experimental Methods of Diagnostics.

\*Member Technical Staff. Member AIAA.

## II. Time-Averaged Raman Signals from Turbulent Flames

Detailed equations for Raman spectral signals from flame gases were listed in the previous study.<sup>14</sup> For vibrational (Q-branch) Raman scattering in laminar flames, a simplified expression for the Raman spectral signal  $S$ , generated by a particular species having a local number density  $n$ , can be written:

$$S = K \cdot F(\lambda, \Delta\lambda, T) \cdot n \quad (1)$$

where  $K$  is a constant which depends on both the experimental system and the species under observation, and  $F(\lambda, \Delta\lambda, T)$  is a dimensionless factor related to the distribution of Raman Q-branch lines within the spectral bandpass of the detection system. The factor  $F$  depends on the spectral resolution  $\Delta\lambda$  and center wavelength  $\lambda$  of the detection system, the local flame temperature  $T$ , and the particular species. Equation (1) indicates that a number density measurement requires a knowledge of the local temperature, a calculation of the factor  $F$  at that temperature, and appropriate calibrations to find the constant  $K$ . The accuracy of the measurement will depend on the accuracy of these individual steps, as well as the statistical uncertainty in the measured Raman signal.<sup>10</sup> If the spectral resolution and center wavelength are chosen so that a particular vibrational band is resolved, an expression for the resulting spectral signal  $S_v$  can be written:

$$S_v = K \cdot \chi(\lambda, \Delta\lambda, T) \cdot n_v \quad (2)$$

where  $n_v$  is the number density of scattering molecules in the vibrational energy state  $v$ , and  $\chi$  is a factor similar to  $F$ . The ratio of spectral signals from two vibrational bands,  $S_v/S_v'$ , is a known function of the local temperature for a diatomic species in thermodynamic equilibrium. Measured values of this ratio can be compared with calculated values to obtain temperature data.

Expressions for time-averaged Raman signals obtained from turbulent flames using a cw-laser spectroscopy system are given by the time averages of the laminar relations in Eqs. (1) and (2). For concentration measurements, Eq. (1) becomes

$$\bar{S} = K \cdot \bar{F}(\lambda, \Delta\lambda, T) \cdot \bar{n} \quad (3)$$

If  $T$  and  $n$  are expressed as sums of mean and fluctuating terms, Eq. (3) can be written:

$$\bar{S} = K \cdot \bar{F}(\lambda, \Delta\lambda, \bar{T}) \cdot \bar{n} \cdot (1 + \epsilon) \quad (4)$$

where the error term  $\epsilon$  is simply:

$$\epsilon = \frac{\bar{F} \cdot \bar{n}}{\bar{F}(\bar{T}) \cdot \bar{n}} - 1 \quad (5)$$

Since the factor  $F$  depends on the spectral resolution and center wavelengths of the detection system, the error  $\epsilon$  also must depend on these parameters. Figure 1 shows the variation of the nitrogen factor  $F$  with temperature for three different spectral bandpasses. The curves show that the variation of  $F$  increases rapidly as the value of the spectral resolution  $\Delta\lambda$  is reduced. Figure 2 shows measured values of  $\bar{F} \cdot \bar{n}$  for nitrogen obtained during the previous study of vertical hydrogen diffusion flames.<sup>14</sup> The number densities in this figure have been normalized by the nitrogen value in room air. The particular flame conditions for these measurements are listed in Table 1. As expected from the corresponding curves in Fig. 1, the measurements in Fig. 2 show a strong dependence on the spectral resolution.

Raman temperature measurements in turbulent flames are obtained from the ratio of time-averaged signals  $\bar{S}_v/\bar{S}_v'$ . Since the two signals typically have temperature dependencies that

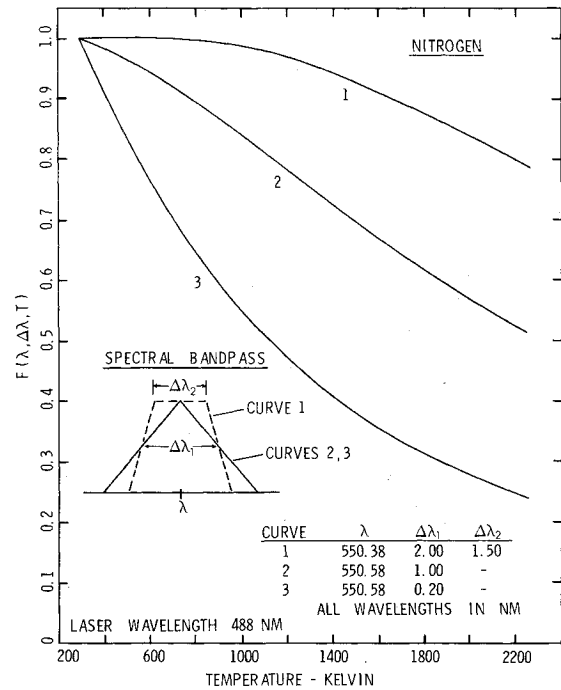


Fig. 1 Calculations of the temperature-dependent factor  $F(\lambda, \Delta\lambda, T)$  for nitrogen.

Table 1 Flame conditions for Raman measurements

Nozzle diameter $d_0$	0.9 mm
Axial position $X/d_0$	50
H <sub>2</sub> velocity at nozzle exit	840 m/s
Froude number	$8.4 \times 10^7$
Reynolds number $(Re)_{d_0}$	6800

are quite different, the ratio of averaged signals probably will not be same as the laminar ratio  $S_v/S_v'$  evaluated at the mean temperature. Thus, a measurement of  $\bar{S}_v/\bar{S}_v'$  generally will not provide an accurate determination of the actual mean temperature. Figure 3 shows temperatures found from ratios of averaged Raman signals obtained during the previous study.<sup>14</sup> Signals were recorded for both vibrational bands from nitrogen and Q-branch lines from hydrogen. The indicated temperatures were found by simply using the laminar expressions for the ratios of these signals.† As shown in Fig. 3, this procedure results in temperatures from hydrogen spectra that are substantially higher than temperatures from nitrogen spectra at each flame position. In order to obtain concentration data from measured values of  $\bar{F} \cdot \bar{n}$ , values of  $\bar{F}(\bar{T})$  must be assumed based on the available temperature data. The curve labeled " $T_a$ " in Fig. 3 shows the temperature values assumed for this purpose in the previous study. The reported profiles of measured mean number densities were found from:

$$\bar{n}_m = \bar{S}/K \cdot \bar{F}(T_a) \quad (6)$$

Using Eq. (4), the ratio of measured mean number density to actual mean number density can be written:

$$\frac{\bar{n}_m}{\bar{n}} = \frac{\bar{F}(\bar{T})}{\bar{F}(T_a)} \cdot (1 + \epsilon) \quad (7)$$

Equation (7) serves to summarize the difficulties in obtaining

†The nitrogen temperatures shown in Fig. 3 are somewhat lower than reported in Ref. 14 due to an error in the previous calculations for  $S_v/S_v'$ .

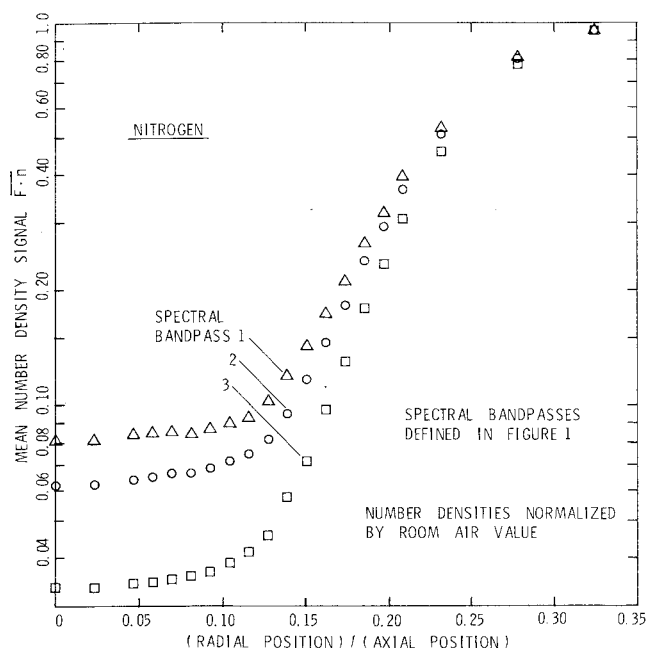


Fig. 2 Raman measurements of time-averaged number density signals in a turbulent hydrogen diffusion flame.<sup>14</sup>

mean flame properties from time-averaged Raman signals. An analysis of errors introduced in averaging pulsed-laser Raman signals from turbulent flames has been given recently by Eckberth.<sup>19</sup>

### III. Direct Determination of Particular Correlations

In the previous section the influence of temperature fluctuations on time-averaged Raman signals was shown to be controlled by the spectral resolution of the detection system. When this result is combined with a simple error analysis for Raman concentration measurements,<sup>14</sup> a procedure can be identified for directly determining certain correlations between fluctuations in temperature and species number density. Experimental data for such correlations would be helpful in formulating turbulent combustion models that incorporate finite-rate chemistry. In these models, correlations between fluctuations in temperature and reactant concentrations are introduced when a global reaction rate in Arrhenius form is time-averaged.<sup>20</sup> Although the analysis in this section is formally restricted to flames in which fluctuations are relatively small, it will be shown that useful information can be obtained even in the severe conditions of a turbulent hydrogen diffusion flame.

A concentration error term  $\epsilon$  was introduced in Eq. (4) in order to relate the time-averaged Raman signal to the actual mean number density. In the previous study<sup>14</sup> a simple analysis was used to examine the sources of this term. If  $T$  and  $n$  are expressed in terms of mean and fluctuating components and  $F$  is expanded in a power series about the mean temperature, then Eq. (5) yields

$$\epsilon(\Delta\lambda) = a_1(\Delta\lambda)t_1 + a_2(\Delta\lambda)t_2 + \dots \quad (8)$$

where

$$a_1 = \frac{\bar{T}}{F(\bar{T})} \frac{dF}{dT}(\bar{T}), \quad a_2 = \frac{\bar{T}^2}{2F(\bar{T})} \frac{d^2F}{dT^2}(\bar{T})$$

$$t_1 = \frac{\overline{n'T'}}{\overline{n \cdot T}}, \quad \text{and} \quad t_2 = \frac{\overline{T'^2}}{\bar{T}^2} + \frac{\overline{n'T'^2}}{\overline{n \cdot T^2}}$$

The dependence of the coefficients  $a_i$  on the spectral resolution  $\Delta\lambda$  follows from the dependence of  $F$  on  $\Delta\lambda$ .

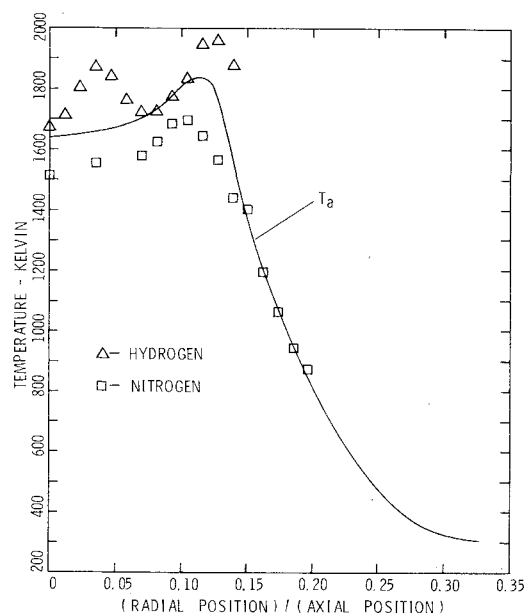


Fig. 3 Raman measurements of mean temperature in a turbulent hydrogen diffusion flame.<sup>14</sup> Temperatures are obtained from both hydrogen and nitrogen spectral signals. The  $T_a$  curve represents estimated mean temperatures used to obtain concentration values from time-averaged number density signals.

Additional terms in the expansion for  $\epsilon$  involve higher-order correlations in  $n'$  and  $T'$ , and higher-order derivatives of  $F$  evaluated at  $\bar{T}$ . If the fluctuations in number density and temperature are relatively small compared to the mean values and the coefficients in the expansion are not large, then the expansion can be truncated after a few terms. At a given flame position the correlations  $t_i$  are unknown constants, while the coefficients  $a_i$  can be calculated provided a good estimate of the mean temperature is available.

If several number density measurements are made at a particular flame position using different spectral resolutions, the error term in the  $i$ th measurement can be expressed in terms of the error in the first measurement as follows:

$$\frac{1 + \epsilon(\Delta\lambda_i)}{1 + \epsilon(\Delta\lambda_1)} = \left[ \frac{F \cdot n}{F(\bar{T})} \right]_{\Delta\lambda_i} \cdot \left[ \frac{F(\bar{T})}{F \cdot n} \right]_{\Delta\lambda_1} \quad (9)$$

Thus, a series of measurements using different spectral resolutions can be used to generate a set of equations containing the unknowns  $\epsilon(\Delta\lambda_1)$ ,  $t_1$ ,  $t_2$ , ...,  $t_N$ . If the expansion for  $\epsilon$  can be truncated after  $N$  terms and a good estimate of the mean temperature is available for coefficient calculations, then a set of  $(N+1)$  equations can be generated and solved to find values for the unknowns  $\epsilon(\Delta\lambda_1)$ ,  $t_1$ ,  $t_2$ , ...,  $t_N$ .

As a test of this procedure, the Raman nitrogen measurements shown in Fig. 2 were used to generate solutions up to  $t_2$  at each flame position. Admittedly, the high fluctuation amplitudes in a hydrogen diffusion flame may represent too severe a flame condition for an accurate evaluation. The coefficients were calculated using the assumed temperature profile  $T_a$  shown in Fig. 3. The maximum amplitude of the coefficients was found to be very near unity. The results of solutions from sets of 3 equations are presented in Fig. 4a. The concentration error  $\epsilon(\Delta\lambda_1)$  is positive throughout the radial profile, with peak values of approximately 0.35 occurring on the rich side of the flame relative to where peak temperatures were recorded (Fig. 3). The first correlation  $t_1$  is negative throughout the radial profile, with peak amplitudes of approximately 0.8. The second correlation  $t_2$  is smaller and negative over most of the profile. The peak values of  $t_2$  are sufficiently large to suggest that additional terms in the expansion for  $\epsilon$  are necessary at

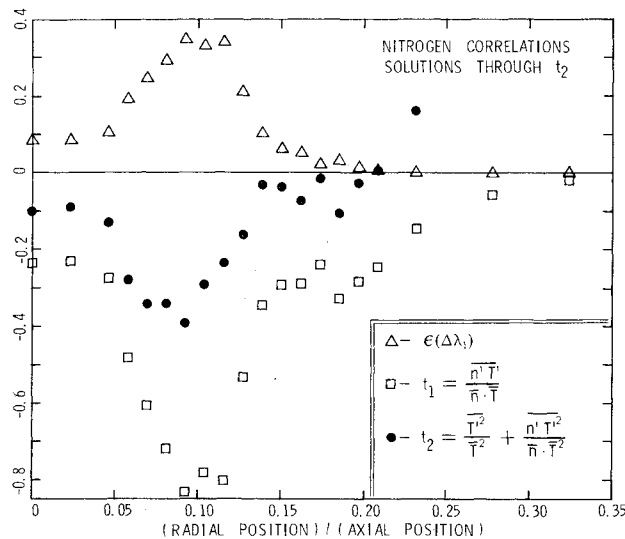


Fig. 4a Nitrogen correlations determined directly from Raman number density signals. The minimum measurement error is also shown.

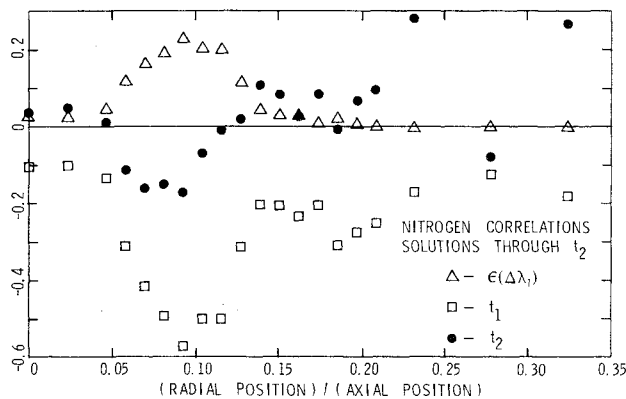


Fig. 4b Nitrogen correlations and minimum measurement error determined from number density signals, with a 3% error assumed in one of the signal calibrations.

these flame positions. Solutions to sets of equations truncated after the  $t_1$  term were also obtained from the pairs of Raman measurements available at each flame position. These results for  $\epsilon(\Delta\lambda_i)$  and  $t_1$  were consistent with the values shown in Fig. 4a except for the flame region where peak values occur. In this region the peak amplitudes were reduced by a factor of approximately 2.

Because of the difficulty in obtaining accurate mean temperatures from time-averaged Raman signals, the sensitivity of the solutions to temperature errors was evaluated. The results showed that solutions to  $t_2$  are quite insensitive to uncertainties in  $\bar{T}$ . For example, if the assumed temperatures are varied  $\pm 100\text{K}$  in the flame region where peak values occur, changes of only a few percent are found in the solutions. A similar examination of the sensitivity to errors in measured Raman signals, however, showed that relatively small errors can have a large effect on the solutions. Figure 4b shows solutions for the same data that were used for the results in Fig. 4a, except that a systematic error of 3% was added to the measurements obtained with a particular spectral bandpass. An error of this magnitude could have been introduced during calibration procedures. The resulting solutions for  $\epsilon(\Delta\lambda_i)$  and  $t_1$  are similar to the solutions shown in Fig. 4a, except that the amplitudes are reduced by 20-40%. The solutions for  $t_2$  have changed significantly, however, with the entire profile shifted toward positive values.

In summary, this test of a procedure for directly determining particular correlations demonstrated that useful

results can be obtained in as severe a flame environment as a turbulent diffusion flame. At a minimum, qualitative values for second-order correlations between temperature and number density fluctuations can be found. The procedure also provides an assessment of the errors introduced in Raman measurements of mean number density. Information on higher-order correlations probably can be found, although this application will require an experimental system capable of providing very accurate measurements of Raman signals.

#### IV. Evaluation of Models for Concentration Fluctuations

A direct approach for examining certain turbulence properties using time-averaged Raman data was presented in the preceding section. A more general approach is to use a set of Raman measurements as a basis for evaluating models for concentration fluctuations in turbulent flames. Two features of Raman measurements suggest that this approach could be quite successful. The first feature, which was utilized in the last section, is that the spectral resolution of the detection system can be used to control how strongly the temperature fluctuations affect the measured signals. The second feature is that the theoretical dependence of Raman signals on the local temperature and number density is precisely known for diatomic molecules. The temperature-dependent factor  $F$  in Eq. (3) can be calculated with excellent accuracy, so a model that predicts how temperature and concentration fluctuations occur at a given flame position will also precisely predict time-averaged Raman signals measured at that position. Comparisons between predicted and measured signals should provide a strong test of the accuracy of the model.

Models for concentration fluctuations are used in diffusion-flame theories which incorporate a number of simplifying assumptions.<sup>21</sup> Chemical rate constants are assumed to be effectively infinite, so local reaction rates are controlled by diffusion. If equal diffusivities of species and thermal energy are assumed, the resulting equations allow the identification of certain scalar functions which are conserved under chemical reaction. Such a conserved scalar was initially used by Burke and Schumann,<sup>22</sup> who assumed a one-step irreversible reaction to derive an infinitely thin "flame-sheet" model. This analysis was first applied to turbulent diffusion flames by Hawthorne et al.<sup>3</sup>, who used a conserved scalar defined to be the local concentration of fluid which originated in the jet nozzle, considering any products present as being decomposed into reactants. Using the flame-sheet assumption, the instantaneous composition was defined by the instantaneous value of the conserved scalar. Time-averaged concentrations were found by weighting the concentrations with a Gaussian probability density function for the conserved scalar. More recent studies have continued to follow this basic approach, with variations suggested for the conserved scalar, for the probability density function of this scalar, and for the reaction model. The conserved scalar used is typically the mixture fraction, which is defined as the local mass fraction of atoms that originated in the jet fluid. Lockwood and Nguib<sup>17</sup> and Elghobashi and Pun<sup>18</sup> reported flame models in which the probability density function is assumed to be a clipped Gaussian bounded by Dirac delta functions at the physical mixture-fraction limits of 0 and 1. Bilger and Kent<sup>15</sup> and Becker<sup>16</sup> replaced the flame-sheet assumption with a shifting-equilibrium reaction model. In this approach the mixture is assumed to be in equilibrium everywhere, with reversible multistep reactions allowed wherever necessary to preserve equilibrium. The local composition and temperature are given by the conditions produced in an adiabatic reaction to equilibrium of premixed fuel and air, with the proportions of the mixture defined by the local mixture fraction. Bilger<sup>21</sup> noted that this reaction model is a better approximation for obtaining temperatures, as well as minor species concentrations.

As an example of how time-averaged Raman measurements can be used to evaluate models for concentration fluctuations,

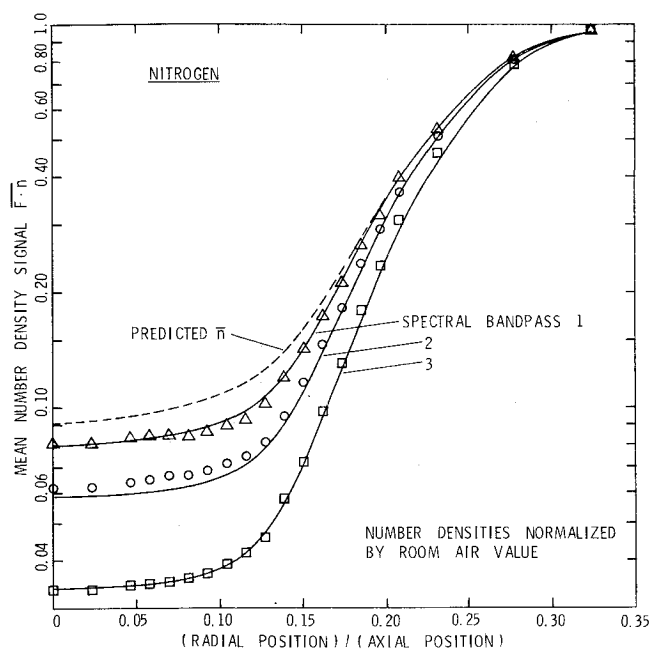


Fig. 5 Predicted values for time-averaged number density signals as fit to measured values.

a combination of the clipped-Gaussian probability density function and the shifting-equilibrium reaction model was used to predict the set of Raman measurements obtained in the previous study.<sup>14</sup> The probability density function  $P$  for the mixture fraction  $f$ , as used by Lockwood and Naguib,<sup>17</sup> is given by

$$P(f) = A\delta(0) + B\delta(1) + \frac{1}{\sigma\sqrt{2\pi}} \exp\left[-\frac{1}{2}\left(\frac{f-\mu}{\sigma}\right)^2\right] \quad (10)$$

where

$$A = \frac{1}{\sigma\sqrt{2\pi}} \int_{-\infty}^0 \exp\left[-\frac{1}{2}\left(\frac{f-\mu}{\sigma}\right)^2\right] df$$

$$B = \frac{1}{\sigma\sqrt{2\pi}} \int_1^{\infty} \exp\left[-\frac{1}{2}\left(\frac{f-\mu}{\sigma}\right)^2\right] df$$

The physically unrealistic "tails" of the Gaussian distribution are put into Dirac delta functions at the physical limits  $f=0,1$ . The value of the  $P(f)$  function at a particular  $f$  is determined by specifying values for the parameters  $\mu$  and  $\sigma$ . In order to predict time-averaged flame properties, values for these parameters must be given at each flame position. Equivalently, values must be specified for the mean mixture fraction  $\bar{f}$  and the variance  $\overline{f'^2}$  at each flame position.† In theoretical flame models utilizing this approach, the mean mixture fraction and the variance are two additional dependent variables whose prediction must be included in the mathematical analysis.<sup>17-18,23</sup> The flame composition and temperature as functions of mixture fraction were found from chemical equilibrium calculations for hydrogen/air using the program of Gordon and McBride.<sup>24</sup> The mean values of flame properties were found by simply integrating the properties over the mixture fraction range using  $P(f)$  as a weighting function. Predicted mean Raman measurements were found in the same fashion using the appropriate relations for  $\bar{S}$  and for  $\overline{S_v}/\overline{S_v}$  (Sec. II).

The method of selecting values for the parameters  $\mu$  and  $\sigma$  at each flame position was somewhat arbitrary. A total of seven profiles of Raman measurements were obtained in the

†Particular values of  $\mu$  and  $\sigma$  uniquely determine corresponding values for the mean mixture fraction and the variance.

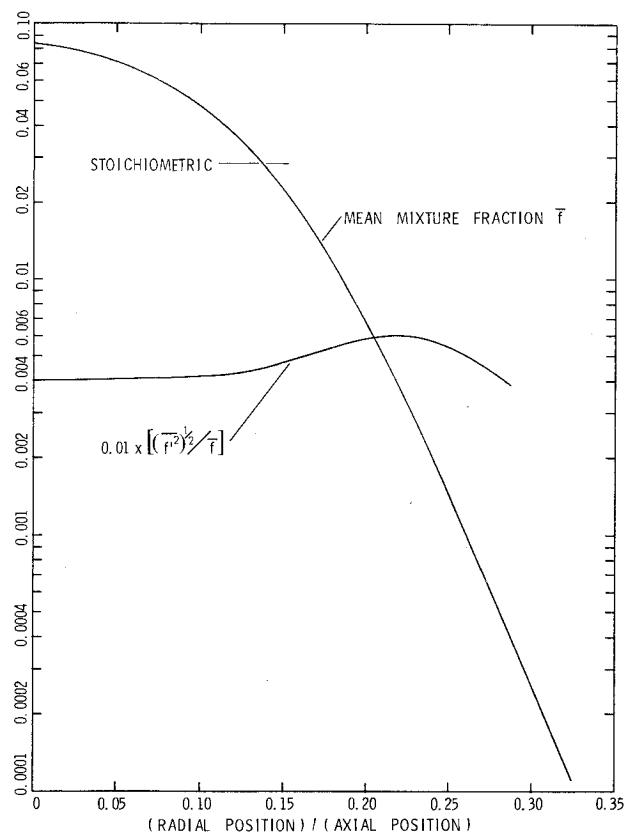


Fig. 6 Mean mixture fraction and the intensity of concentration fluctuations as determined by fitting the nitrogen Raman data.

previous study:  $\overline{F \cdot n}$  data for nitrogen using three different spectral bandpasses,  $\overline{F \cdot n}$  data for oxygen and hydrogen using a single bandpass, and temperature data from ratios of both nitrogen and hydrogen spectral signals. The method chosen was to simply find smooth profiles for  $\mu$  and  $\sigma$  which gave good overall agreement with the  $\overline{F \cdot n}$  data for nitrogen shown in Fig. 2. Emphasis was placed on fitting the two data profiles corresponding to the largest and smallest values of spectral resolution, as these profiles should provide the greatest sensitivity for matching the intensity of the temperature fluctuations. The results of this fitting procedure are shown in Fig. 5. The sensitivity of the fitting was quite good throughout the radial profile, and the resulting values for the mean mixture fraction  $\bar{f}$  and the intensity of concentration fluctuations, defined by  $(\overline{f'^2})^{1/2}/\bar{f}$ , are shown in Fig. 6. The value of the mean mixture fraction at the flame axis, 0.084, agrees very well with the predictions and measurements reported by Kent and Bilger,<sup>23</sup> and the range of intensity values is quite close to the constant value of 0.5 they chose for their calculations.

This fit to the nitrogen data can now be used to predict profiles corresponding to the remaining Raman data. Comparisons between these predictions and measurements will provide the test for the accuracy of the model under evaluation. Figure 7 shows a comparison of predicted and measured  $\overline{F \cdot n}$  values for hydrogen and oxygen. The agreement is quite good for oxygen, but the predicted values for hydrogen are somewhat lower than the measurements. Figure 8 shows a comparison of predicted and measured temperatures, as well as predictions for the actual mean temperature and the intensity of temperature fluctuations. The comparison between measured and predicted temperatures from ratios of nitrogen spectral signals is quite good, with predicted values somewhat higher near the flame axis. However, the predicted values for the actual mean temperature are substantially higher throughout the profile. The problem in obtaining accurate mean temperatures from

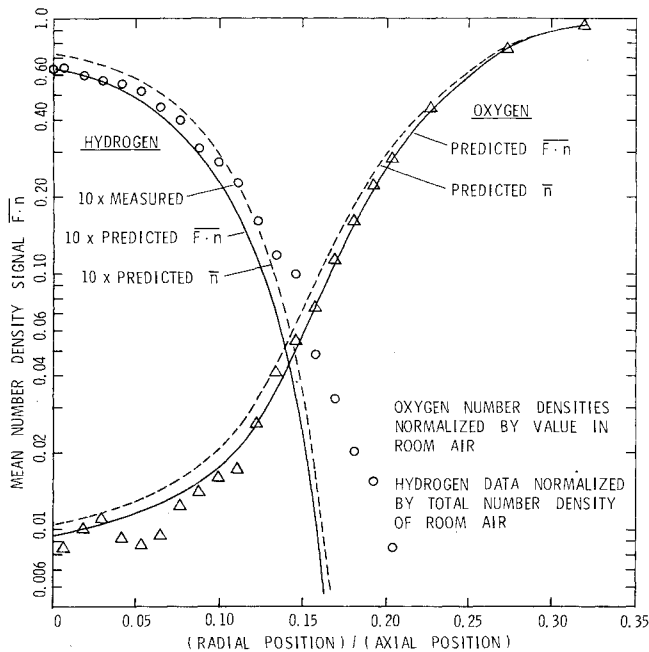


Fig. 7 Predicted and measured number density signals for hydrogen and oxygen.

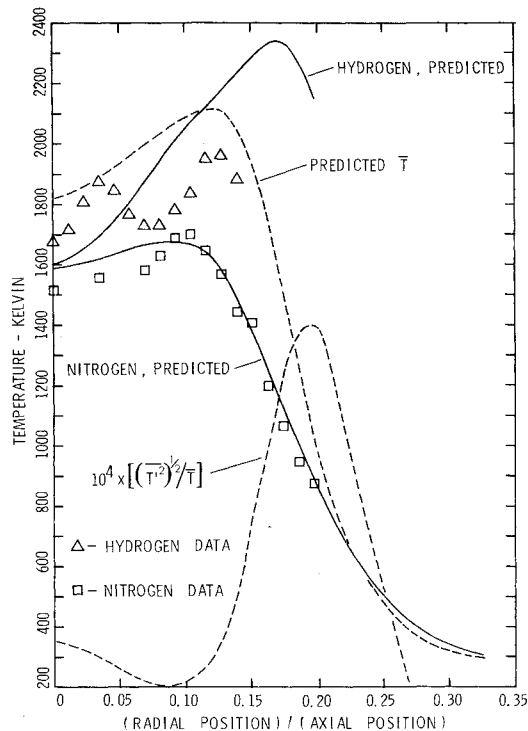


Fig. 8 Predicted and measured temperatures from ratios of time-averaged Raman signals. Predictions for the actual mean temperature and the intensity of temperature fluctuations (dimensionless) are also shown.

ratios of time-averaged Raman signals was identified in Sec. II, but the results shown in Fig. 8 clearly indicate the severity of this problem. The predicted temperatures from ratios of hydrogen spectral signals are higher than the nitrogen temperatures, but show poor agreement with the measured hydrogen temperatures. The measurements show a pronounced, repeatable oscillation in the profile, unlike the smooth predicted profile. The intensity of temperature fluctuations reaches a maximum at a radial position beyond where mean temperatures peak, as observed in a methane

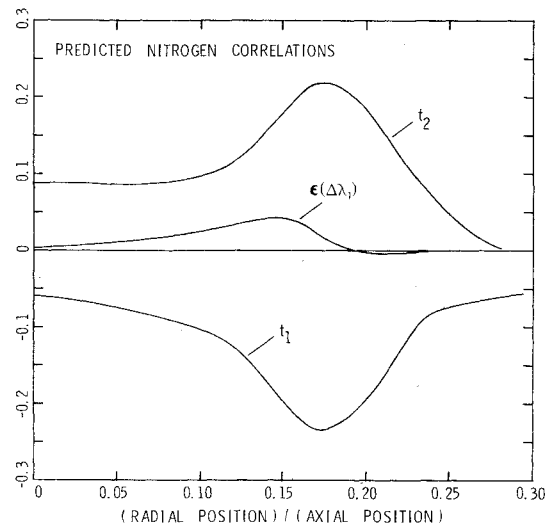


Fig. 9 Predictions of the concentration error  $\epsilon(\Delta\lambda_f)$  and the correlations  $t_1$  and  $t_2$  for nitrogen.

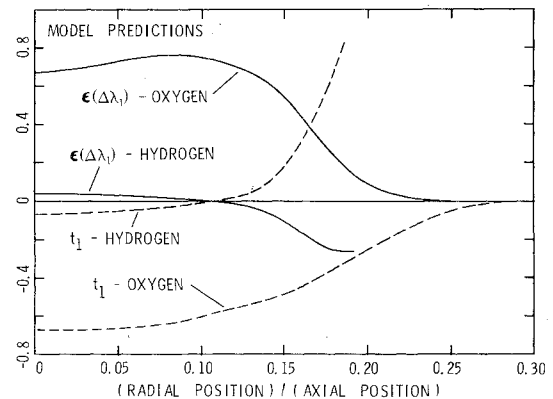


Fig. 10 Predictions of the concentration error  $\epsilon(\Delta\lambda_f)$  and the correlation  $t_1$  for hydrogen and oxygen.

diffusion flame by Lockwood and Odidi.<sup>8</sup> The peak value of the rms temperature fluctuation,  $[T'^2]^{1/2}$ , is predicted to be close to 190 K.

As a final exercise in evaluating this particular model for concentration fluctuations, predictions were made of the concentration error  $\epsilon(\Delta\lambda_f)$  and the correlations  $t_1$  and  $t_2$  as defined in Sec. III. The results for nitrogen are shown in Fig. 9. The predictions for  $\epsilon(\Delta\lambda_f)$  and  $t_1$  are qualitatively similar to the experimental results in Figs. 4a and 4b, although the amplitudes are considerably lower and the peak values occur at larger radial positions. The  $t_2$  correlation is predicted to be positive throughout the radial profile, with an amplitude close to that of  $t_1$ . Similar predictions for oxygen and hydrogen are shown in Fig. 10. The concentration errors for hydrogen are predicted to be quite small. In the experiments and calculations the spectral bandpass was centered on the  $J=3$  Q-branch line of hydrogen, which results in a factor  $F$  that is relatively insensitive to temperature changes. The large concentration errors predicted for oxygen are somewhat misleading. The time-averaged signals  $\bar{F} \cdot \bar{n}$  are found to be very close to the predicted mean number density  $\bar{n}$  for oxygen (Fig. 7). The spectral bandpass resulted in a factor  $F$  that varied rapidly with temperature, so dividing  $\bar{F} \cdot \bar{n}$  by  $F(\bar{T})$  in Eq. (5) produced large values for  $\epsilon$ . The  $t_1$  correlation for oxygen is predicted to be negative and quite large throughout the profile.

The comparisons shown in Figs. 7 and 8 are presented to illustrate this use of Raman data and not to provide a thorough evaluation of the particular model used. In fact, the

model predicted profiles for temperatures from nitrogen and number densities of oxygen quite well, hydrogen number densities fairly well, and hydrogen temperatures poorly. Other fitting procedures could have been chosen which might have resulted in different comparisons. A 3-parameter model to provide a better representation for intermittency<sup>15</sup> might have been a better choice for this initial evaluation, but the fitting procedure would have been more arduous. The comparisons as presented are felt to provide sufficient evidence for the usefulness of this method.

## V. Conclusions

The results of the present study show that time-averaged Raman measurements in turbulent flames can provide useful information on local fluctuations in temperature and composition. In one approach, a simple procedure was identified for determining particular correlations from concentration measurements that are made using different spectral resolutions. This approach appears capable of providing estimates, if not measurements, of some of the correlation terms introduced in finite-rate chemistry models when reaction rates are time-averaged. A more general approach was demonstrated in which a set of time-averaged Raman measurements can be used to evaluate particular models for concentration fluctuations. This method for utilizing Raman data appears to be quite promising. A variety of Raman measurements can be made to provide a large data base for comparisons with model predictions. The different measurements are influenced to different degrees by the fluctuations in temperature and composition, indicating that comparisons will be sensitive to the details of particular models. An appropriate set of careful Raman measurements, obtained over a range of axial and radial positions in a well-defined turbulent diffusion flame, should prove a useful contribution towards improved understanding of these flames.

## Acknowledgments

The author wishes to thank R.W. Bilger for his suggestions on how to examine the effects of local fluctuations on time-averaged Raman signals. The equilibrium calculations used in this study were provided by J.A. Miller. This work was sponsored by the U.S. Department of Energy under Contract DE-AC04-76-DP00789 to Sandia Laboratories, a U.S. Department of Energy facility.

## References

- <sup>1</sup>"Turbulent Reactive Flows," Special Issue edited by F.V. Bracco, *Combustion Science and Technology*, Vol. 13, 1976, pp. 1-275.
- <sup>2</sup>Bilger, R.W., "Turbulent Jet Diffusion Flames," *Progress in Energy and Combustion Science*, Vol. 1, 1976, pp. 87-109.
- <sup>3</sup>Hawthorne, W.R., Weddell, D.S., and Hottel, H.C., "Mixing and Combustion in Turbulent Gas Jets," *Third Symposium on Combustion, Flame, and Explosion Phenomena*, Williams and Wilkins, Baltimore, Md., 1949, pp. 266-300.
- <sup>4</sup>Kent, J.H. and Bilger, R.W., "Turbulent Diffusion Flames," *Fourteenth Symposium (International) on Combustion*, The Combustion Institute, Pittsburgh, Pa., 1973, pp. 615-625.
- <sup>5</sup>Bilger, R.W. and Beck, R.E., "Further Experiments on Turbulent Jet Diffusion Flames," *Fifteenth Symposium (International) on Combustion*, The Combustion Institute, Pittsburgh, Pa., 1975, pp. 541-552.
- <sup>6</sup>Kent, J.H. and Bilger, R.W., "Measurement Techniques in Turbulent Diffusion Flames," Charles Kolling Research Laboratory, University of Sydney, Rept. 243, 1973.
- <sup>7</sup>Lavoie, G.A. and Schlader, A.F., "A Scaling Study of NO Formation in Turbulent Diffusion Flames of Hydrogen Burning in Air," *Combustion Science and Technology*, Vol. 8, 1974, pp. 215-224.
- <sup>8</sup>Lockwood, F.C. and Odidi, A.O.O., "Measurement of Mean and Fluctuating Temperature and of Ion Concentration in Round Free-Jet Turbulent Diffusion and Premixed Flames," *Fifteenth Symposium (International) on Combustion*, The Combustion Institute, Pittsburgh, Pa., 1975, pp. 561-571.
- <sup>9</sup>Lapp, M., "Flame Temperatures from Vibrational Raman Scattering," *Laser Raman Gas Diagnostics*, Plenum Press, New York, 1974, pp. 107-145.
- <sup>10</sup>Setchell, R.E., "Analysis of Flame Emissions by Laser Raman Spectroscopy," Western States Section/The Combustion Institute Paper 74-6, May 1974; also, Sandia Laboratories Report SLL 74-5244, May 1974.
- <sup>11</sup>Setchell, R.E., "Raman Scattering from Laminar and Turbulent Flame Gases," *Combustion Measurements*, Academic Press, New York, 1976, pp. 211-220.
- <sup>12</sup>Stephenson, D.A. and Aiman, W.R., "A Laser Raman Probe of a Premixed Laminar Flame," *Combustion and Flame*, Vol. 31, 1978, pp. 85-88.
- <sup>13</sup>Setchell, R.E. and Miller, J.A., "Raman Scattering Measurements of Nitric Oxide in Ammonia/Oxygen Flames," *Combustion and Flame*, Vol. 33, 1978, pp. 23-32.
- <sup>14</sup>Setchell, R.E., "Time-Averaged Measurements in Turbulent Flames Using Raman Spectroscopy," *AIAA Progress in Astronautics and Aeronautics: Experimental Diagnostics in Gas Phase Combustion Systems*, Vol. 53, New York, 1977, pp. 499-515; also, AIAA Paper 76-28, Jan. 1976.
- <sup>15</sup>Bilger, R.W. and Kent, J.H., "Concentration Fluctuations in Turbulent Jet Diffusion Flames," *Combustion Science and Technology*, Vol. 9, 1974, pp. 25-29.
- <sup>16</sup>Becker, H.A., "Effects of Concentration Fluctuations in Turbulent Diffusion Flames," *Fifteenth Symposium (International) on Combustion*, The Combustion Institute, Pittsburgh, Pa., 1975, pp. 601-615.
- <sup>17</sup>Lockwood, F.C. and Naguib, A.S., "The Prediction of the Fluctuations in the Properties of Free, Round-Jet, Turbulent, Diffusion Flames," *Combustion and Flame*, Vol. 24, 1975, pp. 109-124.
- <sup>18</sup>Elghobashi, S.E. and Pun, W.M., "A Theoretical and Experimental Study of Turbulent Diffusion Flames in Cylindrical Furnaces," *Fifteenth Symposium (International) on Combustion*, The Combustion Institute, Pittsburgh, Pa., 1975, pp. 1353-1365.
- <sup>19</sup>Eckbreth, A.C., "Averaging Considerations for Pulsed, Laser Raman Signals from Turbulent Combustion Media," *Combustion and Flame*, Vol. 31, 1978, pp. 231-237.
- <sup>20</sup>Borghini, R., "Chemical Reactions Calculations in Turbulent Flows: Application to a Co-Containing Turbojet Plume," *Advances in Geophysics*, Vol. 18B, 1974, pp. 349-365.
- <sup>21</sup>Bilger, R.W., "The Structure of Diffusion Flames," *Combustion Science and Technology*, Vol. 13, 1976, pp. 155-170.
- <sup>22</sup>Burke, S.P. and Schumann, T.E.W., "Diffusion Flames," *Industrial and Engineering Chemistry*, Vol. 20, 1928, pp. 998-1004.
- <sup>23</sup>Kent, J.H. and Bilger, R.W., "The Prediction of Turbulent Diffusion Flame Fields and Nitric Oxide Formation," *Sixteenth Symposium (International) on Combustion*, The Combustion Institute, Pittsburgh, Pa., 1977, pp. 1643-1656.
- <sup>24</sup>Gordon, S. and McBride, B.J., "Computer Program for Calculation of Complex Chemical Equilibrium Compositions, Rocket Performance, Incident and Reflected Shocks, and Chapman-Jouguet Detonations," NASA SP-273, 1971.